



# Joint effect of $\beta$ -eutectoid content and heat treatment on the properties of binary Ti-Cu and Ti-Mn alloys

L. Bolzoni<sup>a,\*</sup>, F. Yang<sup>a</sup>, Y. Alshammari<sup>a,b</sup>

<sup>a</sup> School of Engineering, The University of Waikato, Hamilton 3240, New Zealand

<sup>b</sup> Construction and Building Materials, Energy and Building Research Centre, Kuwait Institute for Scientific Research, P.O. Box 24885, Safat 13109, Kuwait

## ARTICLE INFO

### Keywords:

Titanium alloys  
Powder metallurgy  
Blended elemental  
Mechanical properties  
 $\beta$  eutectoid stabiliser

## ABSTRACT

The use of cheap alloying elements and alternative manufacturing techniques are two strategies that can be used to reduce the high cost of Ti alloys. Furthermore, heat treatments are an easy and cost effective method to tailor the mechanical behaviour by means of the modification of the microstructure. For that, this work analysed the quenching and aging heat treatment of binary Ti-Cu and Ti-Mn alloys manufactured via powder metallurgy. It is found that the post-processing solution treatment does not significantly affect the physical properties and residual porosity remains unchanged within the microstructure; however, the heat treatment changes the microconstituents. Serrated martensitic transformed  $\beta$  is formed in quenched Ti-Cu alloys and it is converted into a coarse lamellar or a hypoeutectoid structure as the Cu content increases with the subsequent aging treatment. Aging of the Ti-Mn alloys slightly coarsen the microstructural features where martensite or equiaxed metastable  $\beta$  grains are obtained after quenching. Enhancing of the mechanical behaviour is generally achieved and the solution treatment switches from improving the ductility to increasing the strength and the hardness as the amount of the alloying element increases.

## 1. Introduction

The highest relative mechanical properties, excellent corrosion resistance, biocompatibility, and moderate strength at high temperatures make Ti and its alloys suitable for a variety of applications spanning from aerospace to biomedical [1]. The workforce Ti-6Al-4V alloy is the most known and used amongst the different Ti alloys [2], compositions refer to weight percentage if not otherwise specified. However, Ti alloys are significantly more expensive than other structural metals, limiting their employability. This has sparked investigations on finding alternative  $\beta$  stabiliser to vanadium [3] and niobium [4], due to their high and variable cost, and exploring alternative more efficient manufacturing technique like powder metallurgy. From a cost point of view, Cu and Mn are promising  $\beta$  stabiliser candidates [5,6]. Although casting can be used, the manufacture of binary Ti-Cu and Ti-Mn alloys via powder metallurgy [7–9] offers the advantages of less energy demand, lower reactivity with oxygen, and prevention of alloying elements segregation. Reduction of the residual porosity intrinsic of the simple press and sinter process can easily be obtained through thermomechanical deformation processes like forging, resulting in the improvement of the mechanical behaviour. This can be further changed

via tailoring the microstructural features using a simple heat treatment.

A variety of casting and powder metallurgy methods have been investigated to manufacture binary Ti-Cu and Ti-Mn alloys. These are exemplified by the works of Kikuchi et al. [6] and Zhang et al. [10] and Kim et al. [11] and Fernandes Santos et al. [5], respectively, for binary Ti-Cu and Ti-Mn alloys manufactured via casting and powder metallurgy. In particular, Kikuchi et al. [6] analysed the microstructure and tensile behaviour of cast Ti-(0.5–10)Cu alloys where the yield stress increased and the elongation decreased due to the formation of the eutectoid microstructure. Zhang et al. [10] prepared Ti-(5–10)Cu alloys using hot pressure sintering (850–1050°C, 30 MPa, 2 h, and furnace cooling) achieving similar trends in terms of compressive properties. Kim et al. [11] investigated cast Ti-(5–20)Mn alloys demonstrating that they exhibit higher hardness and better oxidation protection than Ti where a lamellar structure was only found in the Ti-5Mn alloy and the  $\omega$  phase only in the Ti-10Mn alloy. Fernandes Santos et al. [5] manufactured Ti-(8–17)Mn alloys via metal injection moulding showing that the alloys are characterised by a  $\beta$ -type microstructure and the amount of  $\omega$  phase progressively decreases as the amount of Mn increases from 8 % to 13 % [5]. In terms of applications of these alloys, Ti-Cu and Ti-Mn are mainly considered as promising materials for biomedical applications

\* Corresponding author.

E-mail address: [bolzoni.leandro@gmail.com](mailto:bolzoni.leandro@gmail.com) (L. Bolzoni).

<https://doi.org/10.1016/j.jalcom.2024.174510>

Received 3 December 2023; Received in revised form 26 February 2024; Accepted 9 April 2024

Available online 16 April 2024

0925-8388/© 2024 The Authors. Published by Elsevier B.V. This is an open access article under the CC BY license (<http://creativecommons.org/licenses/by/4.0/>).

due to the antibacterial capability of Cu and the biocompatibility of Mn, respectively. For example, Wang et al. [12] clarified the effect of Cu on the mechanical and corrosion properties of cast Ti-(4–10)Cu alloys whilst Bai et al. [13] addressed the biocompatibility of sintered Ti-(10)Cu alloy quantifying the in vivo bone response. Concurrently, Zhang et al. [14] recently proposed new Mn-bearing Ti alloys reporting that the alloys are nontoxic to human osteosarcoma cells in comparison with pure titanium, and Zhou et al. [15] analysed minor Sn modifications of the Ti-(2–4)Mn alloy and the resultant mechanical properties and corrosion behaviour.

Tailoring of the phases for changing the resulting mechanical behaviour through precipitation hardening heat treatments has extensively been studied for cast/wrought binary Ti-Cu and Ti-Mn alloys [16–19]. For example, Hayama et al. [16] analysed the effect of an annealing treatment (900°C/2 h and furnace cooling) as a function of the composition of cast Ti-5Cu (hypoeutectoid), Ti-7.1Cu (eutectoid), and Ti-15Cu (hyper-eutectoid) resulting in the improvement of the ductility of the alloys. Holden et al. [19] quantified the mechanical properties of several Ti-(0.5–12)Mn alloys subjected to different heat treatments including annealing (750°C/1 h) and solution treated (700–750°C/1 h, quenching, and aging 400°C/4 h) showing that the microstructural features have a higher impact on the ductility rather than on the strength of the alloys. The heat treatment of binary Ti-Cu and Ti-Mn alloys manufactured via powder metallurgy has not been extensively investigated and, therefore, there is a lack of knowledge. Consequently, the aim of this study is to analyse the microstructure and quantify the mechanical behaviour of heat treated powder metallurgy  $\beta$  eutectoid bearing Ti alloys (i.e. Ti-Cu and Ti-Mn). In particular, the alloys were prepared using press and sinter of blended elemental powders followed by forging in the  $\beta$  field for their subsequent solution and aging heat treatment.

## 2. Experimental procedure

The raw materials acquired for this study were a Ti powder with maximum particle size < 75  $\mu\text{m}$  and 0.21 % oxygen, a Cu powder with maximum particle size < 63  $\mu\text{m}$  and < 0.10 % oxygen, and a Mn powder with maximum particle size < 45  $\mu\text{m}$  and < 0.10 % oxygen. Particle size

and purity data as per suppliers' specifications. Fig. 1 shows the morphology of the raw powders where it can be seen that the Ti and Mn powders are irregular whilst the Cu powder is dendritic.

The correct ratio of the elemental powders were mixed in a V-shaped blender operated at 30 Hz for 30 min. Specifically, binary Ti-0.5Cu, Ti-2.5Cu, and Ti-5Cu as well as binary Ti-1Mn, Ti-5Mn and Ti-10Mn alloys were analysed. Shaping of the powder blends was done at room temperature by means of uniaxial cold pressing, applying 600 MPa. It is worth mentioning that the compositions were chosen based on the stabilisation power of the alloying elements to cover the full spectrum of Ti alloys, from near- $\alpha$  (i.e. Ti-0.5Cu) to  $\beta$  (i.e. Ti-10Mn). The samples were vacuum sintered at 1250°C for 2 h using a heating rate of 10°C/min, which are common parameters for sintering Ti alloys [15,20–23]. Subsequently, the samples were heated to 1150°C using an induction coil under an argon atmosphere and forged (reduction ratio  $\sim 1.4$ ) using a strain rate in order of  $1 \text{ s}^{-1}$ . Finally, the forged samples were subjected to a solution and aging heat treatment entailing heating to 950°C for 1 h, water quenching, aging at 400°C for 8 h, and final air cooling. It is worth noticing that the chosen forging temperatures are meant to be within the  $\beta$  region for all the alloys according to their respective phase diagrams [24]. It is also worth mentioning that literature [6,16,17,25,26] was used to select the heat treatment conditions. In particular, Zhang et al. [27] heat treated binary Ti-(2–4)Cu alloys obtaining the best compromise between mechanical, biocorrosion and antibacterial properties by means of a solution treatment (900°C/3 h, quenching, and aging at 400°C/12 h). Similarly, Ikeda et al. [28] analysed the response of binary Ti-(6–15)Mn alloys solution treated (900°C/3 h, quenching, and aging at 400/500°C for different times).

The theoretical density was computed using the rule of mixtures. The green density was calculated as the mass to volume ratio. The density of the sintered or forged samples was quantified through water displacement measurements. Porosity is the difference between the density of the forged and fully dense alloys whereas the densification is the difference between the forged and sintered density divided by the difference between the theoretical and sintered density. For microstructural analysis, which was carried out using an Olympus BX60F5 optical microscope, the heat treated samples were ground, polished, and etched

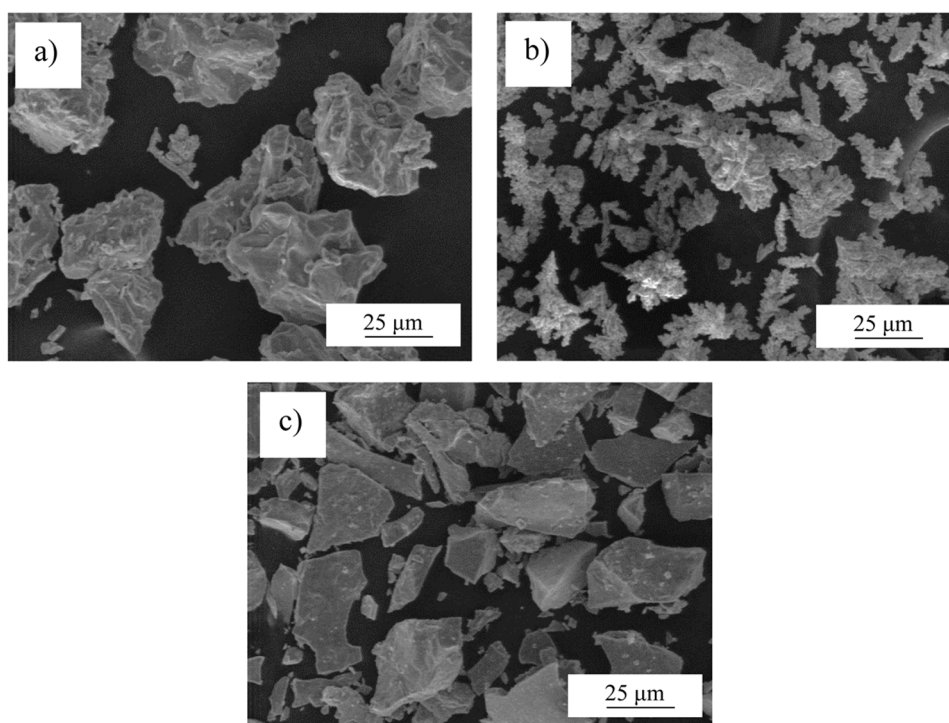


Fig. 1. SEM micrographs showing the morphology of the raw powders: a) Ti, b) Cu, and c) Mn.

(Kroll solution comprising 6 ml  $\text{HNO}_3$ , 2 ml  $\text{HF}$  and 92 ml distilled water). At least three dog-bone shaped samples with  $2 \times 2 \text{ mm}^2$  cross-section and 20 mm gauge length were tested via a computer controlled electro-mechanical universal testing machine (Instron 33R4204) applying a strain rate of  $5 \cdot 10^{-3} \text{ s}^{-1}$ . The offset method was used to determine the yield stress and a mechanical extensometer was used to measure the elongation. A minimum of five Vickers hardness indentations were performed to subsequently evaluate the average hardness of the alloys.

### 3. Results and discussion

The variation of the physical properties of the investigated binary Ti-Cu and Ti-Mn alloys including density, porosity, and densification are shown in Fig. 2. It can be seen that the theoretical density of the alloys linearly increases with the amount of alloying elements from  $4.53 \text{ g/cm}^3$  to  $4.73 \text{ g/cm}^3$  for the Ti-Cu alloys and from  $4.54 \text{ g/cm}^3$  to  $4.80 \text{ g/cm}^3$  for the Ti-Mn alloys. These values are higher than the density of Ti (i.e.  $4.51 \text{ g/cm}^3$ ) and it is due to the fact that both Cu (i.e.  $8.96 \text{ g/cm}^3$ ) and Mn (i.e.  $7.43 \text{ g/cm}^3$ ) are heavier than Ti. In comparison, the theoretical density of the Ti-Mn alloys is higher than that of the Ti-Cu alloys despite the lower density of Mn due to the greater amount of Mn used in the binary alloys with respect to Cu. Concerning the green density, its value monotonically decreases, with comparable slope, with the amount of alloying elements for the addition of either Cu or Mn due to the reduced compressibility of the powder blends (Fig. 2a). This is, respectively, related to the dendritic morphology of the Cu powder and the higher hardness of the Mn powder on top of the difference in terms of maximum

particle size. The Ti-Mn alloys powder blends have slightly higher relative compressibility as a consequence of the smaller particle size and more favourable powder particle morphology. The density of both sintered and forged samples linearly increases with the amount of Cu or Mn. However, it is noticeable the remarkably much higher slope at which the sintered density of the binary Ti-Cu alloys increases with respect to the other cases.

A more in depth insight on the specific effect of the alloying element powders used is obtained by analysing the variation of the relative sintered density values vs. the green density (Fig. 2b). The green density decreases in both systems, from 83.7 % to 79.5 % and from 85.1 % to 79.2 %, respectively, for Ti-Cu and Ti-Mn alloys. The higher values of the latter alloys, where the alloying element content is greater, is related to their better compressibility. The sintered density increases from 89.2 % to 93.5 % with the amount of Cu whereas decreases from 94.5 % to 91.2 % with the Mn content. Therefore, higher values of sintered density are achieved for higher additions of Cu even though the green density decreases. Conversely, the sintered density of Ti-Mn alloys decreases with the amount of Mn despite the better compressibility. As all the specimens were sintered under the same conditions, this is related to the intrinsic diffusivity of each alloying element which is higher for Cu due to its lower melting point in comparison to Mn. However, because of the higher green density, generally higher sintered density values are found for the binary Ti-Mn alloys. It is worth mentioning that the relative sintered density values reported in Fig. 2b) are comparable to those of other Ti-based materials manufactured by press and sinter [5,29–33].

From Fig. 2c), the density of the forged Ti-Cu alloys initially increases (i.e. 98.8–99.6 %) and then decreases (i.e. 98.7 %) with the

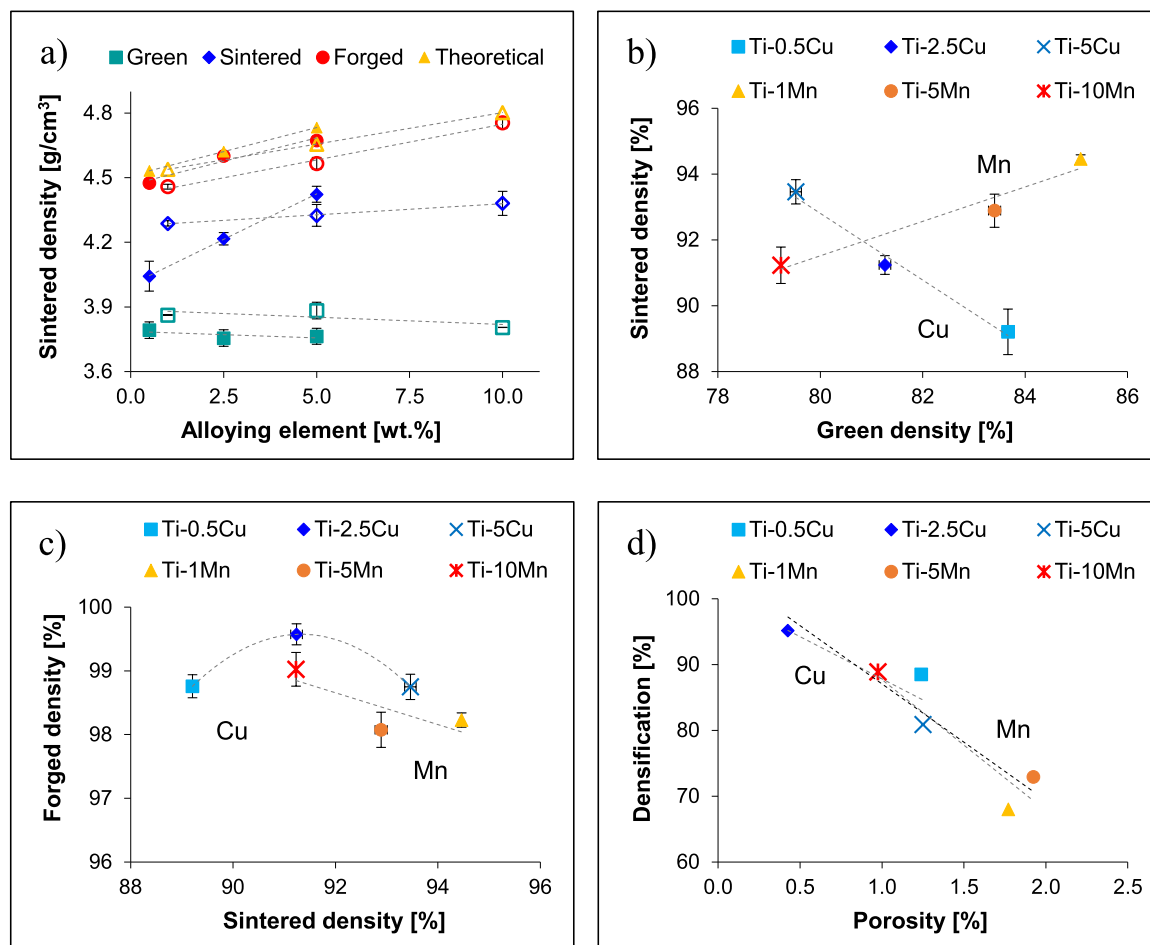


Fig. 2. Variation of the physical properties of the binary Ti-Cu and Ti-Mn alloys: a) sintered density vs. amount of alloying element (note: full symbols are for Ti-Cu alloys and empty symbols are for Ti-Mn alloys), b) sintered density vs. green density, c) forged density vs. sintered density, and d) densification vs. porosity.

amount of Cu, which is directly correlated with the increase in sintered density induced by the addition of Cu. The forging density values are higher with respect to the sintered samples, meaning that hot forging is successful in sealing the majority of the residual porosity. However, the gap between the two values decreases (i.e. 9.6–5.3 %) as the content of Cu increases, indicating that the alloy becomes less plastically deformable. In the case of the Ti-Mn alloys, the forging density increases (i.e. 98.2–99.0 %) with the amount of Mn, which corresponds to a linear decrement with the sintered density. Consequently, the difference between the two monotonically increases (i.e. 3.8–7.8 %) with the Mn content, implying a better deformability for greater Mn additions. Generally, higher forging density values are achieved in the binary Ti-Cu alloys with respect to the Ti-Mn alloys despite the former having lower sintered density, suggesting that Ti-Cu alloys are more comparatively malleable than Ti-Mn alloys. The combination of the behaviours previously discussed results in the binary Ti-Cu alloys having overall higher densification and lower amount of residual porosity after hot forging with respect to their binary Ti-Mn counterparts (Fig. 2d). For both systems, as it could have been expected, higher densifications are associated with lower porosity values resulting in an overall decreasing trend common to both types of alloys.

Fig. 3 shows representative micrographs of the quenched and aged

Ti-Cu alloys. Those of the sintered and forged samples are available elsewhere [8]. However, as the final microstructure of Ti alloy depends on the overall thermal history, the sintered Ti-Cu alloys are characterised by the classical lamellar microstructure composed of  $\alpha$  grain boundaries and  $\alpha+\beta$  lamellae. As the amount of Cu increases, the size of the  $\alpha+\beta$  lamellae is progressively refined and a hypoeutectic structure of  $\alpha$ -Ti lamellae and  $\text{Ti}_2\text{Cu}$  intermetallic phase [34] that transforms from  $\beta$ -Ti at the eutectoid temperature is found in the Ti-5Cu alloy. The forged Ti-Cu alloys have a martensitic-like microstructure due to the fast cooling experienced by the material during forging. The fineness of the martensitic structure uniformly increases with the amount of Cu. It is worth mentioning that contrary to binary Ti alloys in which the eutectoid reaction is sluggish (e.g. Ti-Mn), the  $\beta$  phase is not retained at room temperature upon water quenching in binary Ti-Cu alloys [17]. A serrated martensitic transformed  $\beta$  microstructure is, therefore, obtained upon quenching in the Ti-Cu alloys regardless of the Cu content. Nonetheless, the coarseness of the transformed  $\beta$  microstructure remarkably decreases moving from the Ti-0.5Cu alloy (Figs. 3a) to Ti-2.5Cu (Fig. 3c) and to Ti-5Cu (Fig. 3e).

Decomposition of the martensite obtained through quenching from the  $\beta$  field is expected to undergo during the aging treatment at 400°C. Fig. 3b) shows that the microstructure of the Ti-0.5Cu alloy is

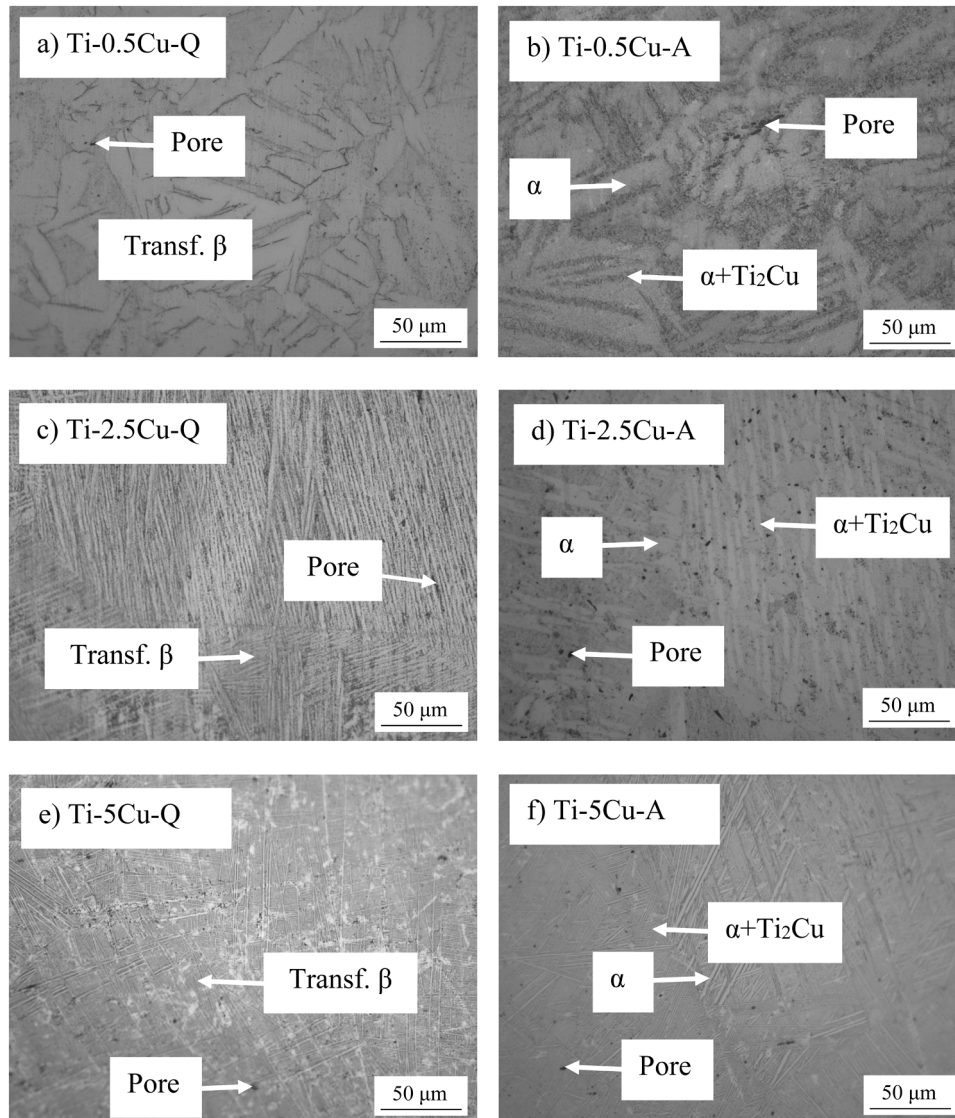


Fig. 3. Representative micrographs of the, respectively, quenched and aged Ti-Cu alloys: a-b) Ti-0.5Cu, c-d) Ti-2.5Cu, and e-f) Ti-5Cu.



constituted by a coarse lamellar structure similar to that obtained upon cooling from the sintering temperature. As 0.5 wt % of Cu is below the maximum solubility of Cu in the  $\alpha$  phase, the microstructure is primarily composed of  $\alpha$  phase grains and a relatively small amount of transformed structure is found at the grain boundaries. In the case of the aged Ti-2.5Cu (Fig. 3d) and Ti-5Cu alloys (Fig. 3b) a microstructure composed of  $\alpha$  grains and the  $\text{Ti}_2\text{Cu}$  phase in the form of lamellae is achieved as a consequence of the decomposition of martensite. The microstructure is commonly found in hypoeutectoid Ti-Cu alloys. Smaller and fewer  $\alpha$  grains and coarser and more regions with the eutectoid  $\alpha\text{-Ti}+\text{Ti}_2\text{Cu}$  structure are present as the Cu content increases. A small amount of either elongated or spherical pores are also present in the microstructure of the quenched and aged Ti-Cu alloys in agreement with the data of Fig. 2 for the forged alloys.

The results of the microstructural characterisation performed on the quenched and aged Ti-Mn alloys are presented in Fig. 4. To understand them, it is worth remembering that a coarse and fine lamellar microstructure was, respectively, found in the Ti-1Mn and Ti-5Mn alloys whereas equiaxed  $\beta$  grains with fine elongated retained  $\alpha$  grains found at the grain boundaries and within some grains were observed for the Ti-10Mn alloy. After forging, an extremely fine lamellar microstructure was found in the Ti-1Mn alloy whilst a fully  $\beta$  microstructure was

obtained in the Ti-5Mn and Ti-10Mn alloys [9]. As for the Ti-Cu alloys, some few small elongated residual pores with either spherical or elongated morphology are also found in the microstructure of the quenched and aged Ti-Mn alloys. Retention of  $\beta$  as a metastable phase is expected in quenched Ti-Mn alloys for a sufficiently high amount of Mn (i.e. 3 %) due to the sluggish eutectoid reaction. Accordingly,  $\alpha'$  martensite forms upon quenching in the Ti-1Mn alloy (Fig. 4a) whilst a microstructure composed of equiaxed metastable  $\beta$  grains is formed in the Ti-5Mn and Ti-10Mn alloys. However, it can be seen that acicular grains originating from martensite are also present, as reported in literature [28]. In this case, the precipitation of such acicular grains is related to the oxygen content which virtually shift the phase transformation temperature to higher values and affects the transformation kinetics. It is, therefore, found that the size of the equiaxed metastable  $\beta$  grains is coarser and that of the acicular grains much finer in the case of the Ti-10Mn alloy.

Aging of the quenched Ti-Mn alloys at 400°C for 8 h does not lead to major modifications of the microstructure, if not to a minor coarsening of the phases. Exclusively in the case of the Ti-1Mn alloy the decomposition of martensite leads to the precipitation of some  $\alpha$  grains resulting in a lookalike lamellar microstructure.

Fig. 5 shows representative examples of the tensile stress-strain curves of the quenched and aged binary Ti-Cu and Ti-Mn alloys. With

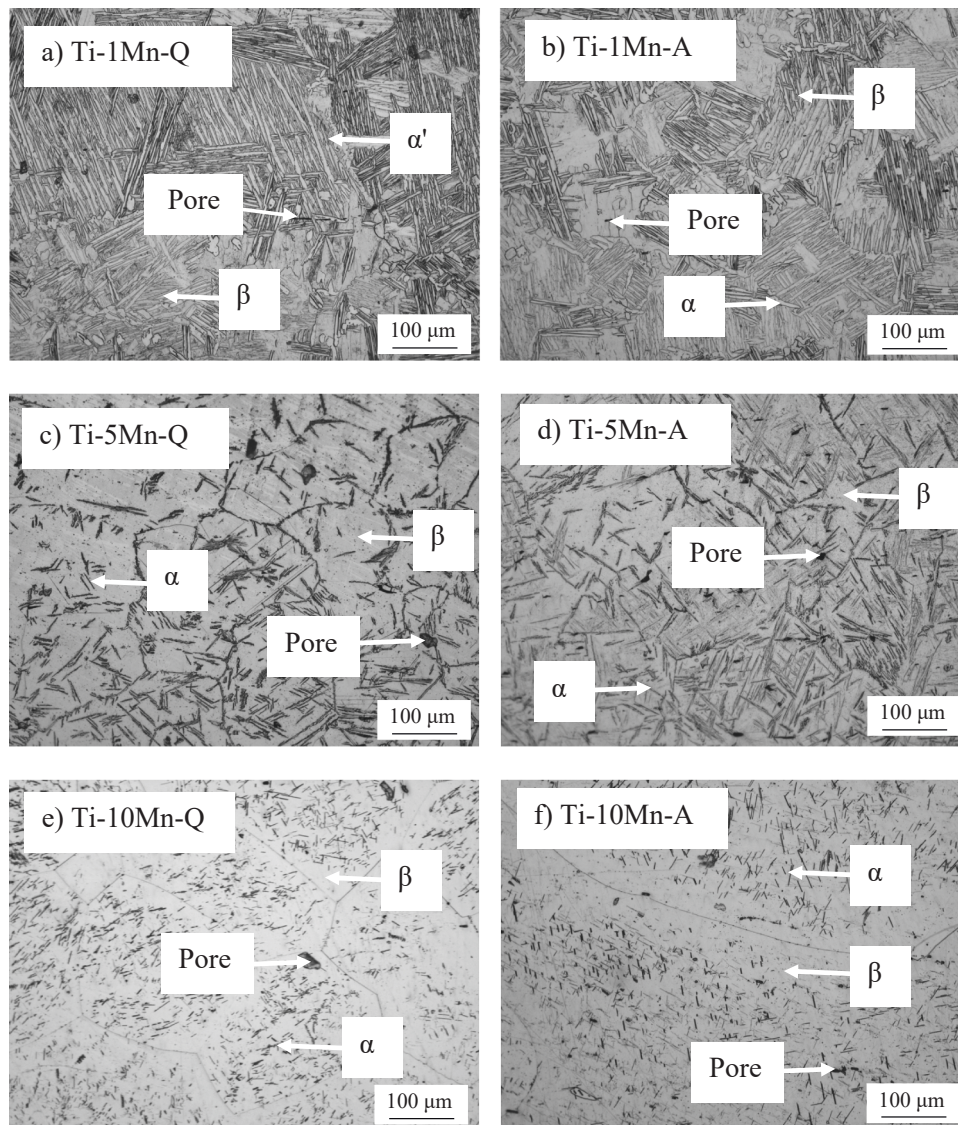
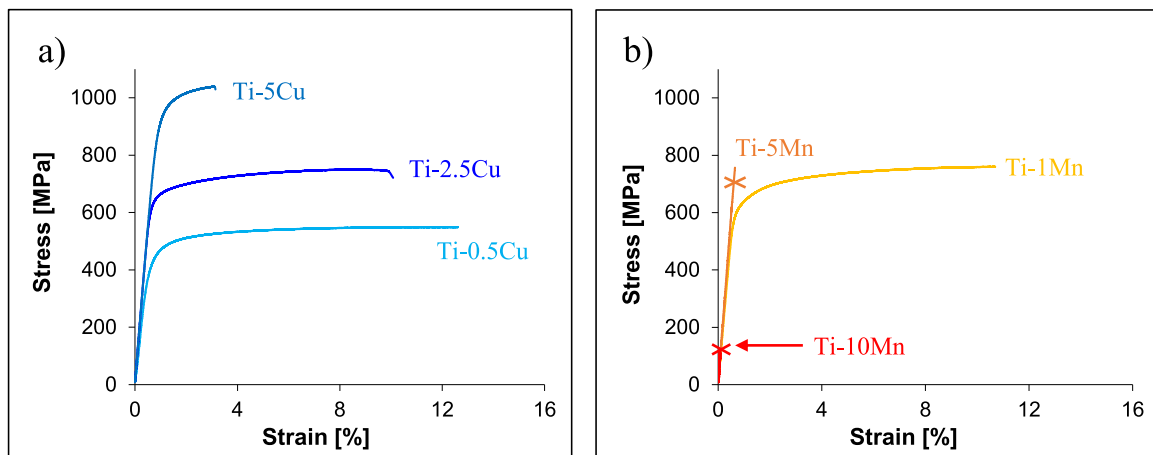


Fig. 4. Representative micrographs of the, respectively, quenched and aged Ti-Mn alloys: a-b) Ti-1Mn, c-d) Ti-5Mn, and e-f) Ti-10Mn.



**Fig. 5.** Representative results of the tensile and hardening behaviour of the quenched and aged binary Ti-Cu and Ti-Mn alloys: a) stress-strain curves of the Ti-Cu alloys, and b) stress-strain curves of the Ti-Mn alloys.

regards to the former, irrespective of their chemistry, the alloys are able to undergo both elastic and plastic deformation before non-catastrophic failure. The stress at which each specific alloy transitions from one behaviour to the other increases with the amount of Cu. Consequently, the resistance to the applied uniaxial tensile load increases but the ability to withstand plastic deformation decreases (Fig. 5a). Similar behaviour and trend could have been expected for the Ti-Mn alloys. However, it can be seen that both the Ti-5Mn and Ti-10Mn alloys only undergo elastic deformation before catastrophic failure whilst the Ti-1Mn alloy is able to plastically deform after the initial elastic deformation. The Ti-Mn alloys become significantly more brittle as the amount of Mn increases.

The strain hardening curves calculated from the true stress vs. true strain derived from the tensile curves of Fig. 5 are displayed in Fig. 6. The depicted  $d\sigma/d\varepsilon_p$  curves are commonly divided between Stage II (i.e. the initial asymptotic part of the curve) and Stage III [35]. In the former, each alloy shows very high  $d\sigma/d\varepsilon_p$  values and a sharp decrease over a narrow plastic strain range where for polycrystalline materials this is not a proper deformation stage [36]. Stage III is characterised by a much slower decrease of the  $d\sigma/d\varepsilon_p$  ratio, which is determined by the dislocation generation to annihilation balance. The type of microstructure and the fineness of its features determines the shape of the  $d\sigma/d\varepsilon_p$  curve. Therefore, it can be seen that the Ti-5Cu alloy has much higher  $d\sigma/d\varepsilon_p$  values in Stage II with respect to the other aged Ti-Cu alloys as a consequence of its very fine hypoeutectoid microstructure (Fig. 3). The

transition from Stage II to Stage III also roughly coincides with the intersection between the  $d\sigma/d\varepsilon_p$  curves of the Ti-0.5Cu and Ti-2.5Cu alloys where the hardening rate of the latter starts to decrease at a faster rate compared to the former (Fig. 6a). In the case of the Ti-Mn alloys, only the  $d\sigma/d\varepsilon_p$  curve of the Ti-1Mn alloy could be derived due to the brittle nature of the aged Ti-5Mn and Ti-10Mn alloys. The Ti-1Mn alloy is characterised by a hardening behaviour, which is comparable to that of the Ti-5Cu alloy in Stage II and to that of the Ti-2.5Cu alloy in Stage III.

The graphs of Fig. 6 also report the variation of the true stress vs. true strain tensile curves where the crossover of these curves with the respective  $d\sigma/d\varepsilon_p$  curves is identified as the onset of necking following the necking stability Considère criterion [37]. It can be seen that there is a strong dependency of the onset of necking value with Stage III and an increase in uniform elongation follows necking upon tensile loading. This relates well with the elastoplastic behaviour of the alloys and it is an estimation of their toughness (Fig. 5). For the binary Ti-Cu alloys, the amount of plastic deformation underwent after necking progressively decreases with the Cu content due to transformation and refinement of the microstructural features (Fig. 3). The necking onset and subsequent deformation of the Ti-1Mn alloy is comparable to that of the Ti-2.5Cu alloy, although of the differences in microstructure.

The average mechanical properties of the quenched and aged binary Ti-Cu alloys as a function of the Cu content are shown in Fig. 7. The yield stress and the ultimate tensile strength both monotonically increase with

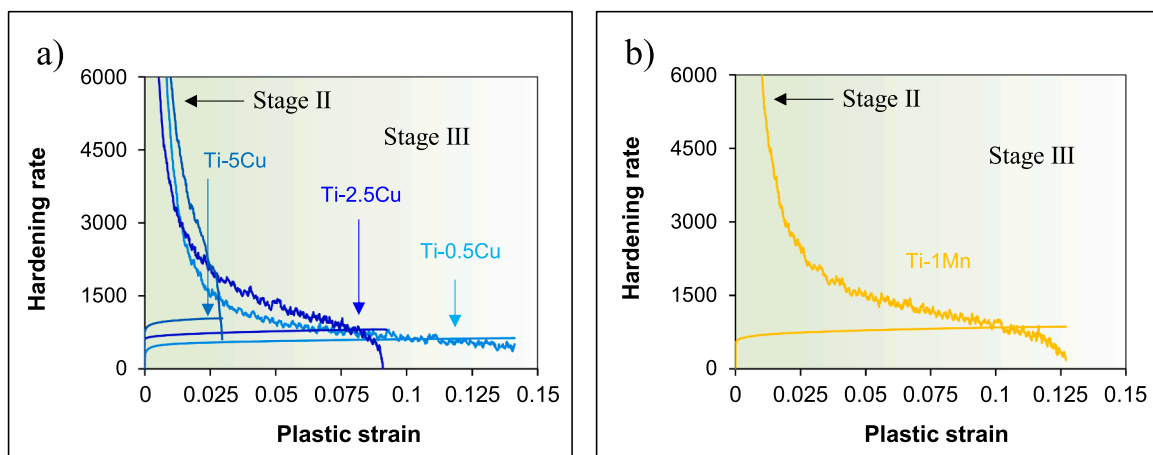


**Fig. 6.** Representative results of the hardening behaviour of the quenched and aged binary Ti-Cu and Ti-Mn alloys: a) strain hardening curves of the Ti-Cu alloys, and b) strain hardening curves of the Ti-Mn alloys.

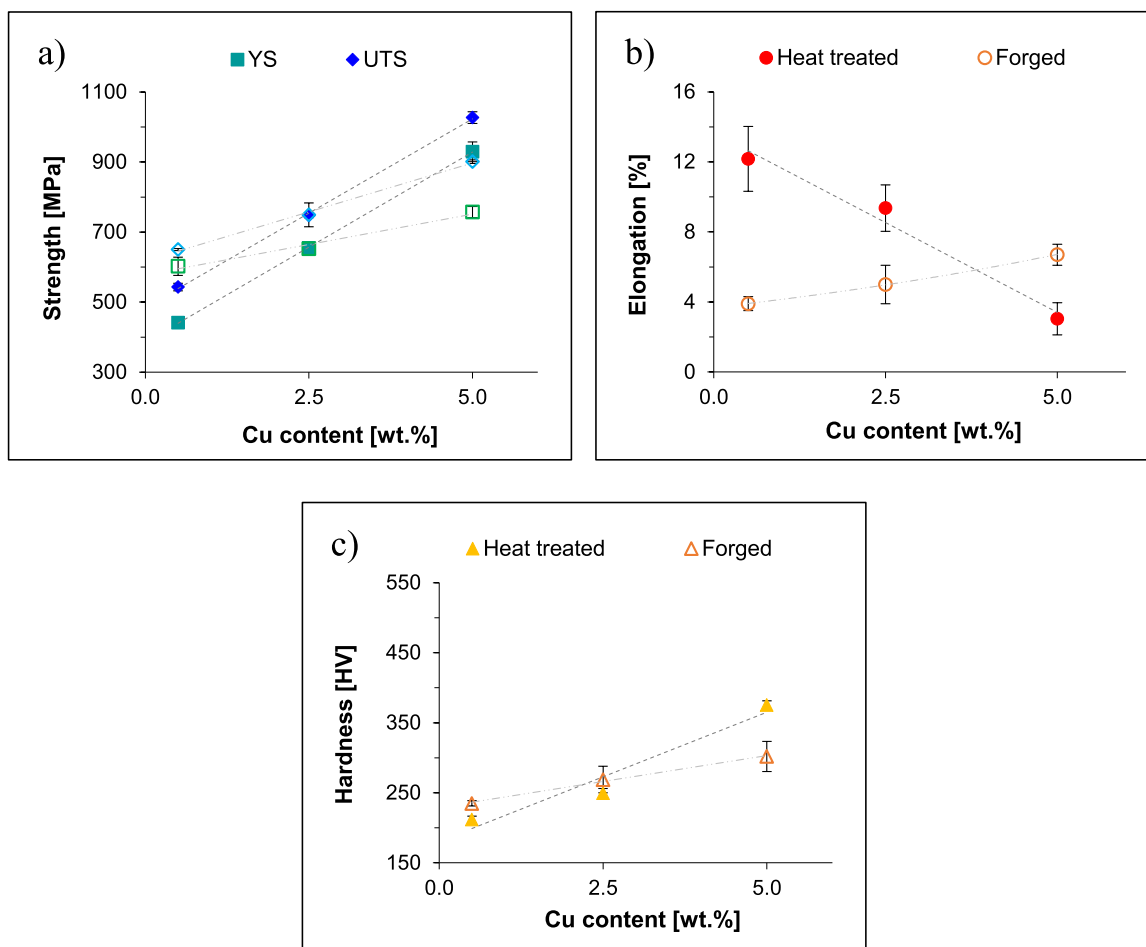


**Fig. 7.** Average mechanical properties of the forged and heat treated binary Ti-Cu alloys: a) yield stress and ultimate tensile strength (note: full symbols are for the heat treated alloys and empty symbols are for forged alloys), b) elongation to fracture, and c) hardness.

the amount of Cu. Specifically, the yield stress increases from 441 MPa to 929 MPa and the ultimate tensile strength from 543 MPa to 1027 MPa. For the sake of comparison, Fig. 7a) also reports the data of the forged alloys [8]. It is found that the selected solution treatment is primarily beneficial to enhance the tensile properties of the Ti-5Cu alloy as the yield stress and the ultimate tensile strength are, respectively, 172 MPa and 126 MPa higher compared to the forged alloy. In the case of the Ti-2.5Cu alloy the heat treatment does not lead to any significant improvement as both the yield stress and the ultimate tensile strength values of the forged and heat treated alloys are comparable. Conversely, for the Ti-0.5Cu alloy, the selected solution treatment decreases both the yield stress and the ultimate tensile strength of 161 MPa and 107 MPa, respectively.

From Fig. 7b), the solution treatment leads to a linear decrease of the elongation to fracture from 12.2 % to 3.0 % as the amount of Cu present in the alloy increases. When compared to the respective forged alloys, it can be seen that the solution plus aging treatment is beneficial to improve the ductility of the binary Ti-Cu alloys; however, its efficacy decreases as the Cu content increases. Therefore, the elongation of the heat treated Ti-0.5Cu alloy is threefold that of the forged counterpart whereas the elongation of the heat treated Ti-5Cu alloy is twice as low as that of the forged alloy. As it could have been expected from the trend of the strength, the solution treatment continuously increases the hardness of the Ti-Cu alloys from 212 HV to 376 HV (Fig. 7c). Once again, the selected heat treatment is beneficial for the Ti-5Cu alloy, neutral for the Ti-2.5Cu alloy and detrimental for the hardness of the Ti-0.5Cu alloy. The changes in mechanical properties induced by the heat treatment and with respect to the forged alloys are due to two main factors, namely the

formation of a progressively refined microstructure during the aging treatment and the creation of the hypoeutectoid structure entailing the presence of the hard but brittle  $\text{Ti}_2\text{Cu}$  intermetallic phase (Fig. 3).

Fig. 8 shows the mean mechanical properties of the quenched and aged binary Ti-Mn alloys as a function of the amount of Mn added. Due to the brittle nature of the alloys, only the yield stress of the Ti-1Mn could be calculated as  $643 \pm 19$  MPa, which is comparable to that of the forged alloy, i.e.  $648 \pm 16$  MPa. The ultimate tensile strength of the aged alloys slightly increases from 752 MPa of the Ti-1Mn alloy to 796 MPa of the Ti-5Mn alloy and then plummets to 108 MPa for the Ti-10Mn alloy (Fig. 8a). A similar increasing and then decreasing trend is found for the forged alloys. The studied solution treatment marginally increases the yield stress of the forged Ti-1Mn alloy by 24 MPa but remarkably decreases that of the other Ti-Mn alloys due to their embrittlement [38]. Interestingly, the studied heat treatment also leads to a slight increase of the ductility of the Ti-1Mn alloy of approximately 1 %. In terms of elongation to failure (Fig. 8b), the heat treated Ti-Mn alloys are characterised by an exponentially decreasing trend as the ductility drops from 10.2 % to 0.6 %. Consequently, the ductility of the Ti-Mn alloys is generally lower after the heat treatment.

Regarding the hardness (Fig. 8c), the solution treatment initially leads to a remarkable increase ( $265 \rightarrow 521$  HV) and subsequently to a much lower one (i.e. 534) as the content of Mn increases. The same trend is found for the forged alloys. It can be noticed that the hardness of the heat treated Ti-Mn alloys is always higher in comparison to their forged counterparts and the gap between the two increases as the Mn content increases. The mechanical behaviour discussed and the extraordinary differences between the various Ti-Mn alloys are related to their

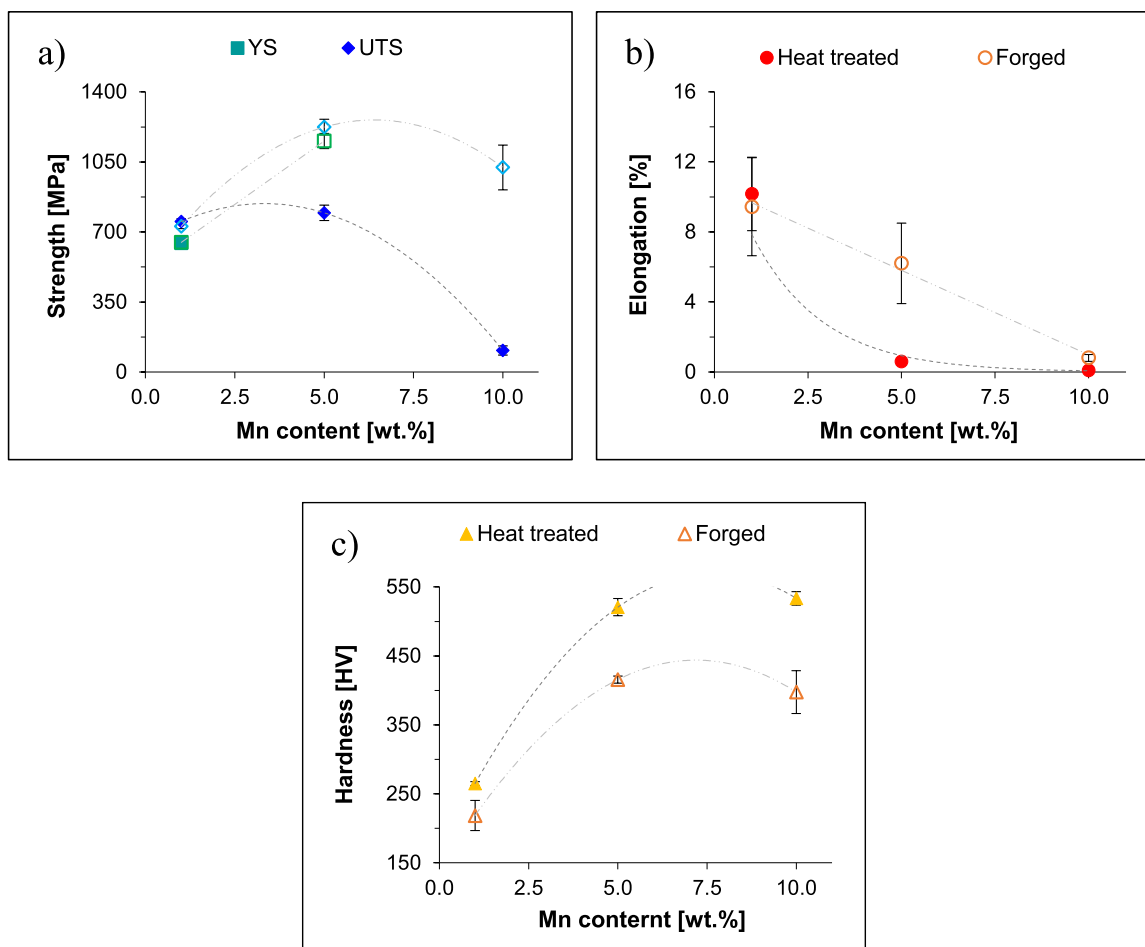


**Fig. 8.** Average mechanical properties of the forged and heat treated binary Ti-Mn alloys: a) yield stress and ultimate tensile strength (note: full symbols are for the heat treated alloys and empty symbols are for forged alloys), b) elongation to fracture, and c) hardness.

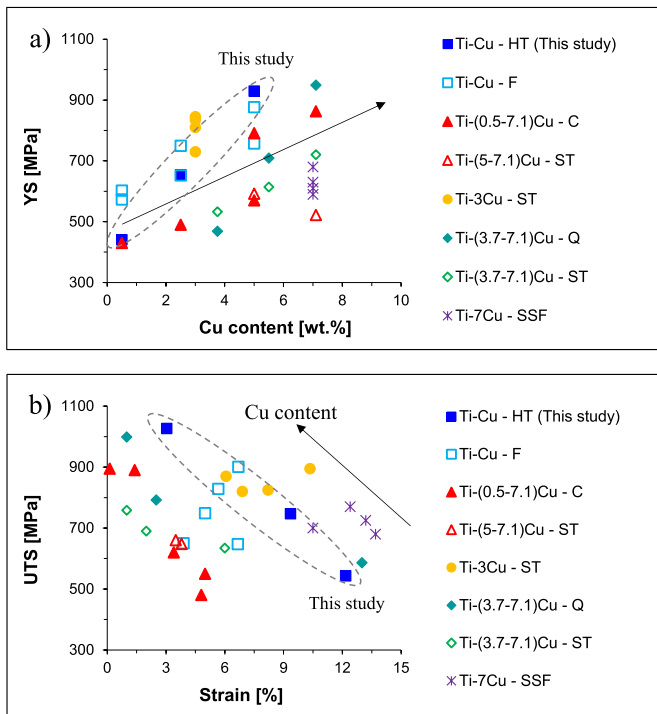
microstructure, which is lamellar for the Ti-1Mn alloy and composed of equiaxed  $\beta$  grains with acicular  $\alpha$  grains for the rest of the alloys (Fig. 4). A direct comparison between the average mechanical properties of the Ti-Cu (Fig. 7) and Ti-Mn (Fig. 8) alloys indicates that the latter are much stronger, harder and less ductile but the results of the strength are biased by their brittleness.

A comparison of the tensile properties of the forged and heat treated Ti-Cu alloys of this study with other binary Ti-Cu alloys manufactured using a variety of methods including post-processing heat treatments [6, 16, 17, 25, 39, 40] is shown in Fig. 9. In general, the yield stress of the binary Ti-Cu alloys increases with the amount of Cu added and the forged and heat treated alloys of this study sit at the up end of the distribution for comparable compositions. Specifically, the yield stress of the heat treated Ti-0.5Cu alloy is lower compared to its forged counterparts but it is slightly higher with respect to that of an equivalent cast alloy. The heat treated Ti-2.5Cu alloy has comparable yield stress to the forged alloys and it is much better with respect to the same alloy obtained via casting (Fig. 9a). Moreover, the yield stress is lower compared to a solution treated Ti-3Cu, as different heat treatments including T4 and T6 for longer times were used, but much better than that of a quenched as well as solution treated Ti-3.7Cu alloy despite the latter bearing a higher Cu content and having been aged at a higher temperature for longer times. Concerning the heat treated Ti-5Cu alloy, it has the best yield stress amongst other Ti-5Cu alloys subjected to forging, casting, quenching or a solution treatment. Furthermore, the Ti-5Cu alloy is characterised by the highest yield stress, better than that of Ti-7.1 Cu alloy manufactured via casting, semisolid forging and solution treated.

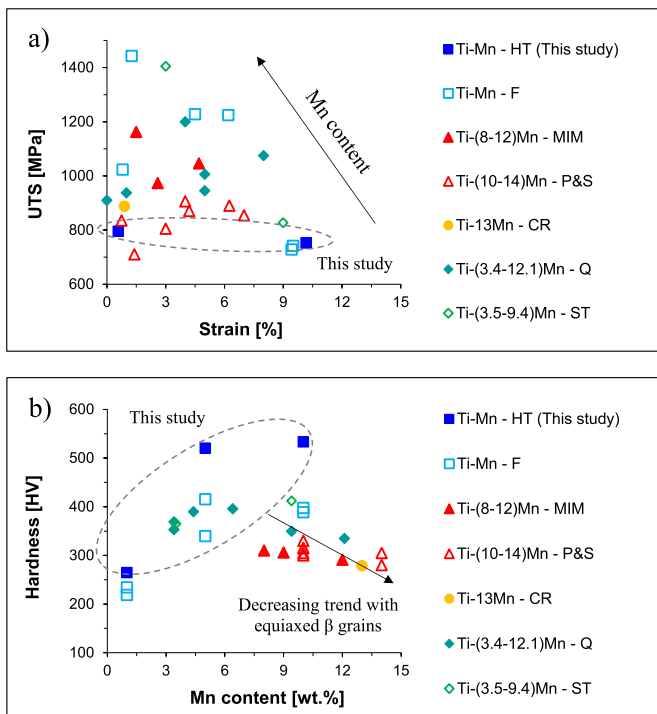
From Fig. 9b), as the ultimate tensile strength increases the ductility decreases and this is generally associated with the increment of the Cu content in the alloy. In terms of UTS/strain pairs, the binary Ti-Cu alloys of this study significantly outperform all the cast and solution treated Ti-(0.5–7.1)Cu alloys as well as the quenched and solution treated Ti-(3.7–7.1)Cu alloys. The heat treated Ti-0.5Cu alloy is amongst those with the best ductility but its strength is, understandably, lower than that of semisolid forged Ti-7Cu alloys and the quenched Ti-3.7Cu alloy due to the lower Cu content. Similarly, the heat treated Ti-2.5Cu alloy has higher strain values than most of the solution treated Ti-3Cu alloys but its ultimate tensile strength is comparatively lower. The highest UTS value is achieved in the heat treated Ti-5Cu alloy combined with better ductility with respect to other Ti-Cu alloy with similar chemical compositions.

Fig. 10 shows a comparison of the mechanical properties of the forged and heat treated Ti-Mn alloys of this study with other binary Ti-Mn alloys obtained by means of different manufacturing methods without and with subsequent heat treatment [5, 19, 40–42]. As for the Ti-Cu alloys, better ductility is associated with lower values of ultimate tensile strength, which are commonly attained in lean compositions. Consequently, the forged and heat treated Ti-1Mn alloy is characterised by the highest elongation to fracture value amongst all the binary Ti-Mn alloys considered (Fig. 10a). Furthermore, its ultimate tensile strength is not remarkably different from that of some of the Ti-Mn alloys obtained via press and sinter. The forged Ti-Mn alloys are the one generally characterised by the best compromise between high ultimate tensile strength and good ductility. Analysing the variation of the hardness with the Mn content (Fig. 10b), the heat treated Ti-Mn alloys have the highest





**Fig. 9.** Comparison of the average tensile properties of the heat treated Ti-Cu alloys with literature [6,16,17,25,39,40]: a) yield stress versus Cu content, and b) ultimate tensile strength versus strain. Legend: HT-heat treated, F-forged, C-cast, ST-solution treated, Q-quenched, and SSF-semisolid forged.



**Fig. 10.** Comparison of the average mechanical properties of the heat treated Ti-Mn alloys with literature [5,19,40–42]: a) ultimate tensile strength versus strain, and b) hardness versus Mn content. Legend: HT-heat treated, F-forged, MIM-metal injection moulded, P&S-pressed and sintered, CR-cold rolled, Q-quenched, and ST-solution treated.

hardness amongst other alloys with comparable chemical composition. Moreover, their hardness is also remarkably higher with respect to alloys bearing a significantly higher amount of Mn such as quenched and solution treated Ti-(3.4–12.1)Mn alloys, metal injection moulded Ti-(8–12)Mn alloys and pressed and sintered Ti-(10–14)Mn alloys. Generally higher hardness values are achieved for higher Mn contents; however, a decreasing sub-trend can also be identified for Mn compositions above a specific threshold, which corresponds to the formation of a microstructure composed of fully stabilised equiaxed  $\beta$  grains.

#### 4. Conclusions

This work investigated the effects that a quenching and aging heat treatment have on the properties and performance of binary Ti-Cu and Ti-Mn alloys manufactured via powder metallurgy, as there is lack of knowledge. From it, the following conclusions can be drawn:

- The theoretical density of the binary Ti-Cu and Ti-Mn alloys monotonically increases with the amount of alloying elements as they are heavier than Ti whilst the green density linearly decreases as the addition of the Cu and Mn powders affects the compressibility of the powder blends. Sintering and forging of the alloys always leads to a progressively higher values for higher alloying elements additions. Due to its higher diffusivity, the addition of Cu is more beneficial in terms of increasing the relative sintered density and forging is effective in sealing most of the residual pores. The subsequent heat treatments do not significantly affect the residual pores, which remain within the microstructure.
- Quenching of the binary Ti-Cu alloys does not results in the retention of the  $\beta$  phase, a serrated martensitic transformed  $\beta$  microstructure is formed, which becomes remarkably finer as the Cu content in the alloy increases. This in turn affects the outcome of the aging treatment and, thus, a coarse lamellar structure is obtained if the Cu content is below the maximum solubility limit. A hypoeutectoid structure composed of  $\alpha$  grains and the intermetallic  $Ti_2Cu$  phase is otherwise created. Conversely, retained  $\beta$  is present in the quenched Ti-Mn alloys and, therefore,  $\alpha'$  martensite is formed for compositions below the maximum solid solubility of Mn and equiaxed metastable  $\beta$  grains for compositions above. Precipitated acicular  $\alpha$  grains are also found. Aging does not change the nature of the microstructure but leads to a minor coarsening of the phases.
- The heat treated alloys are generally characterised by an elastoplastic tensile behaviour, which becomes purely elastic for the binary Ti-Mn alloys as the Mn content increases. Accordingly, the yield stress and the ultimate tensile strength monotonically increase, and so does the hardness, and the elongation to fracture linearly decreases as the alloying element content increases. Furthermore, the alloys are characterised by similar overall strain hardening behaviour, but the details of the strain hardening curve depend on the type of microstructure and the fineness of its features, with the majority of the alloys sustaining plastic deformation after the onset of necking. The solution treatment transitions from enhancing the ductility to improving the strength and the hardness as the amount of the alloying element increases. Nevertheless, the actual amount of improvement of each property is highly dependent on the chemical composition of each specific binary Ti-Cu and Ti-Mn alloy.
- The heat treated Ti-5Cu alloy is characterised by the highest yield stress amongst alloys with comparable composition but manufactured using different methods and the binary Ti-Cu of this study significantly outperform all the cast, quenched, and solution treated alloys in terms of UTS/strain pairs. The best ductility among all the compared binary Ti-Mn alloys is obtained in the heat treated Ti-1Mn alloy and the highest hardness values are achieved in the heat treated Ti-Mn alloys.

## CRediT authorship contribution statement

**Leandro Bolzoni:** Investigation, Conceptualization, Methodology, Writing – review & editing. **F. Yang:** Methodology. **Y. Alshammari:** Methodology, Investigation.

## Declaration of Competing Interest

The authors declare no conflict of interest.

## Data availability

All metadata pertaining to this work will be made available on reasonable requests.

## Acknowledgements

This research did not receive any specific grant from funding agencies in the public, commercial, or not-for-profit sectors. The authors would like to acknowledge the technical contribution of Mr. Hao Liu.

## References

- [1] G. Lütjering, J.C. Williams, *Titanium: Engineering Materials and Processes*, first ed., Springer, Manchester, UK, 2003.
- [2] C. Leyens, M. Peters, *Titanium and Titanium Alloys. Fundamentals and Applications*, Wiley-VCH, Köln, Germany, 2003.
- [3] L. Bolzoni, P.G. Esteban, E.M. Ruiz-Navas, E. Gordo, Mechanical behaviour of pressed and sintered titanium alloys obtained from prealloyed and blended elemental powders, *J. Mech. Behav. Biomed. Mater.* 14 (2012) 29–38.
- [4] L. Bolzoni, M. Paul, F. Yang, Effect of combined lean additions of isomorphous and eutectoid beta stabilisers on the properties of titanium, *J. Mater. Res. Technol.* 21 (2022) 3828–3843.
- [5] P. Fernandes Santos, M. Niinomi, H. Liu, K. Cho, M. Nakai, Y. Itoh, T. Narushima, M. Ikeda, Fabrication of low-cost beta-type Ti-Mn alloys for biomedical applications by metal injection molding process and their mechanical properties, *J. Mech. Behav. Biomed. Mater.* 59 (2016) 497–507.
- [6] M. Kikuchi, Y. Takada, S. Kiyosue, M. Yoda, M. Woldu, Z. Cai, O. Okuno, T. Okabe, Mechanical Properties and Microstructures of Cast Ti-Cu alloys, *Dent. Mater.* 19 (3) (2003) 174–181.
- [7] M. Qian, F.H. Froes, *Titanium Powder Metallurgy - Science, Technology and Applications*, Butterworth-Heinemann, Oxford, U.K., 2015.
- [8] Y. Alshammari, F. Yang, L. Bolzoni, Low-cost powder metallurgy Ti-Cu alloys as a potential antibacterial material, *J. Mech. Behav. Biomed. Mater.* 95 (2019) 232–239.
- [9] Y. Alshammari, F. Yang, L. Bolzoni, Mechanical properties and microstructure of Ti-Mn alloys produced via powder metallurgy for biomedical applications, *J. Mech. Behav. Biomed. Mater.* 91 (2019) 391–397.
- [10] E. Zhang, S. Li, J. Ren, L. Zhang, Y. Han, Effect of extrusion processing on the microstructure, mechanical properties, biocorrosion properties and antibacterial properties of Ti-Cu sintered alloys, *Mater. Sci. Eng. C* 69 (2016) 760–768.
- [11] J.-W. Kim, M.-J. Hwang, M.-K. Han, Y.-G. Kim, H.-J. Song, Y.-J. Park, Effect of manganese on the microstructure, mechanical properties and corrosion behavior of titanium alloys, *Mater. Chem. Phys.* 180 (2016) 341–348.
- [12] Z. Wang, B. Fu, Y. Wang, T. Dong, J. Li, G. Li, X. Zhao, J. Liu, G. Zhang, Effect of Cu content on the precipitation behaviors, mechanical and corrosion properties of As-Cast Ti-Cu alloys, *Materials* 15 (5) (2022) 1696.
- [13] B. Bai, E. Zhang, H. Dong, J. Liu, Biocompatibility of antibacterial Ti-Cu sintered alloy: in vivo bone response, *J. Mater. Sci. Mater. Med.* 26 (12) (2015) 265, 12p.
- [14] H. Zhang, C. Wang, F. Pyczak, T. Ebel, X. Liu, A new kind of biomedical Ti-Mn-Nb alloy, *Phys. Status Solidi (a)* 220 (7) (2023) 2200348.
- [15] X. Zhou, H. Fang, T. Yuan, R. Li, Effect of slight Sn modification on mechanical properties and corrosion behavior of Ti- (2–4 wt %) Mn alloys fabricated via powder metallurgy, *Mater. Charact.* 203 (2023) 113068.
- [16] A.O.F. Hayama, P.N. Andrade, A. Cremasco, R.J. Contieri, C.R.M. Afonso, R. Caram, Effects of composition and heat treatment on the mechanical behavior of Ti-Cu alloys, *Mater. Des.* 55 (2014) 1006–1013.
- [17] F.C. Holden, A.A. Watts, H.R. Ogden, R.I. Jaffee, Heat treatment and mechanical properties of Ti-Cu alloys, *JOM* 7 (1) (1955) 117–125.
- [18] H.R. Ogden, F.C. Holden, R.I. Jaffee, Effect of alpha solutes on the heat-treatment response of Ti-Mn alloys, *JOM* 7 (1) (1955) 105–112.
- [19] F.C. Holden, H.R. Ogden, R.I. Jaffee, Heat treatment, structure, and mechanical properties of Ti-Mn alloys, *JOM* 6 (2) (1954) 169–184.
- [20] S. Raynova, Y. Collas, F. Yang, L. Bolzoni, Advancement in the pressureless sintering of CP titanium using high-frequency induction heating, *Metall. Mater. Trans. A* 50 (10) (2019) 4732–4742.
- [21] A. Amigó-Mata, M. Haro-Rodríguez, Á. Vicente-Escuder, V. Amigó-Borrás, Development of Ti-Zr alloys by powder metallurgy for biomedical applications, *Powder Metall.* 65 (1) (2022) 31–38.
- [22] M.T. Jia, B. Gabbitas, L. Bolzoni, Evaluation of reactive induction sintering as a manufacturing route for blended elemental Ti-5Al-2.5Fe alloy, *J. Mater. Process. Technol.* 255 (2018) 611–620.
- [23] T. Sjafrizal, A. Dehghan-Manshadi, D. Kent, M. Yan, M.S. Dargusch, Effect of Fe addition on properties of Ti-6Al-xFe manufactured by blended elemental process, *J. Mech. Behav. Biomed. Mater.* 102 (2020) 103518.
- [24] J.L. Murray, *Phase Diagrams of Binary Titanium Alloys*, first ed., ASM International 1987.
- [25] M. Bao, Y. Liu, X. Wang, L. Yang, S. Li, J. Ren, G. Qin, E. Zhang, Optimization of mechanical properties, biocorrosion properties and antibacterial properties of wrought Ti-3Cu alloy by heat treatment, *Bioact. Mater.* 3 (1) (2018) 28–38.
- [26] X. Yao, Q.Y. Sun, L. Xiao, J. Sun, Effect of Ti2Cu precipitates on mechanical behavior of Ti-2.5Cu alloy subjected to different heat treatments, *J. Alloy. Compd.* 484 (1) (2009) 196–202.
- [27] E. Zhang, J. Ren, S. Li, L. Yang, G. Qin, Optimization of mechanical properties, biocorrosion properties and antibacterial properties of As-cast Ti-Cu alloys, *Biomed. Mater.* 11 (6) (2016) 065001.
- [28] M. Ikeda, M. Ueda, R. Matsunaga, M. Ogawa, M. Niinomi, Isothermal aging behavior of beta titanium-manganese alloys, *Mater. Trans.* 50 (12) (2009) 2737–2743.
- [29] L. Bolzoni, E.M. Ruiz-Navas, E. Gordo, Powder metallurgy CP-Ti performances: hydride-dehydride vs. sponge, *Mater. Des.* 60 (2014) 226–232.
- [30] D. Zhao, K. Chang, T. Ebel, M. Qian, R. Willumeit, M. Yan, F. Pyczak, Microstructure and mechanical behavior of metal injection molded Ti-Nb binary alloys as biomedical material, *J. Mech. Behav. Biomed. Mater.* 28 (2013) 171–182.
- [31] B.-Y. Chen, K.-S. Hwang, K.-L. Ng, Effect of cooling process on the alpha phase formation and mechanical properties of sintered Ti-Fe alloys, *Mater. Sci. Eng. A* 528 (2011) 4556–4563.
- [32] S. Ehtemam-Haghighi, H. Attar, M.S. Dargusch, D. Kent, Microstructure, phase composition and mechanical properties of new, low cost Ti-Mn-Nb alloys for biomedical applications, *J. Alloy. Compd.* 787 (2019) 570–577.
- [33] L. Bolzoni, M. Alqattan, L. Peters, Y. Alshammari, F. Yang, Ternary Ti alloys functionalised with antibacterial activity, *Sci. Rep.* 10 (1) (2020) 22201.
- [34] C. Ohkubo, I. Shimura, T. Aoki, S. Hanatani, T. Hosoi, M. Hattori, Y. Oda, T. Okabe, Wear resistance of experimental Ti-Cu alloys, *Biomaterials* 24 (2003) 3377–3381.
- [35] F. Geng, M. Niinomi, M. Nakai, Observation of yielding and strain hardening in a titanium alloy having high oxygen content, *Mater. Sci. Eng.: A* 528 (16–17) (2011) 5435–5445.
- [36] U.F. Kocks, H. Mecking, Physics and phenomenology of strain hardening: the FCC case, *Prog. Mater. Sci.* 48 (3) (2003) 171–273.
- [37] L. Weber, M. Kouzeli, C. San Marchi, A. Mortensen, On the use of Considere's criterion in tensile testing of materials which accumulate internal damage, *Scr. Mater.* 41 (5) (1999) 549–551.
- [38] M.K. Gouda, K. Nakamura, M.A.H. Gepreel, Effect of Mn-content on the deformation behavior of binary Ti-Mn Alloys, *Key Eng. Mater.* 705 (2016) 214–218.
- [39] C. Yongnan, H. Yazhou, Z. Yiping, S. Xuding, Z. Yongqing, B. Zhaozhao, L. Liao, Effect of Cu content on the semi-solid formability and mechanical properties of Ti-Cu alloys, *Rare Met. Mater. Eng.* 45 (6) (2016) 1406–1412.
- [40] Y. Alshammari, M. Jia, F. Yang, L. Bolzoni, The effect of  $\alpha + \beta$  forging on the mechanical properties and microstructure of binary titanium alloys produced via a cost-effective powder metallurgy route, *Mater. Sci. Eng.: A* 769 (2020) 138496.
- [41] K. Cho, M. Niinomi, M. Nakai, J. Hieda, P. Fernandes Santos, Y. Itoh, M. Ikeda, Mechanical properties, microstructures, and biocompatibility of low-cost  $\beta$ -type Ti-Mn alloys for biomedical applications, *Biomater. Sci. Process., Prop. Appl.* IV 251 (2014) 21–30.
- [42] K. Cho, M. Niinomi, M. Nakai, H. Liu, P.F. Santos, Y. Itoh, M. Ikeda, M.A.-H. Gepreel, T. Narushima, Improvement in mechanical strength of low-cost  $\beta$ -type Ti-Mn alloys fabricated by metal injection molding through cold rolling, *J. Alloy. Compd.* 664 (2016) 272–283.